Electron temperature measurements from line-to-continuum ratios in hydrogen laser-induced plasma

CHRISTIAN G. PARIGGER

Physics and Astronomy Department, University of Tennessee, University of Tennessee Space Institute,
Center for Laser Applications, 411 B.H. Goethert Parkway, Tullahoma, TN 37388-9700, USA
E-mail: cparigge@tennessee.edu

ABSTRACT: Recent experiments on laser-induced optical breakdown in hydrogen gas investigate the line-to-continuum temperature diagnostic to characterize expanding laser-plasma. Each of the four members of the Balmer series, namely, $H\alpha$, $H\beta$, $H\gamma$, and $H\delta$ lines, delivers electron temperature from the integrated line to 10-nm continuum radiation. This work communicates $H\gamma$ and $H\delta$ for diagnostic applications. This work also discusses comparisons with standard Boltzmann plots that require at least $H\alpha$ and $H\beta$, over and above the establishment of local thermodynamic equilibrium. The experiments employ a 150 mJ, 6 ns Q-switched Nd:YAG laser device operated at the fundamental wavelength of 1064 nm. A 0.64-m spectrometer with an attached gated detector records the emission from the plasma with a spectral system resolution of 0.1 nm. The temperatures from all four Balmer lines are in the range of 90 kK to 40 kK for time delays from plasma initiation in the range of 75 ns to 275 ns, respectively, and agree within error bars.

PACS Codes: 52.70.-m, 32.30-r, 52.25.Jm, 42.62.Fi

Keywords: Plasma diagnostics, atomic spectra, plasma spectroscopy, laser spectroscopy, laser-induced breakdown spectroscopy.

1. INTRODUCTION

Laser-induced optical breakdown of gases causes initially a shock-wave dominated plasma expansion. The shock wave is described by the Taylor-Sedov model [1]. Laser spectroscopy of the hydrogen plasma utilizes the full-width half maximum (FWHM) of Stark-broadened, spectral line shapes [2-6] for evaluation of electron density. The electron density, N_e, can be determined from the FWHM even in cases for which local thermodynamic equilibrium is not yet established [7]. This work aims to find the electron temperature, T_e, from a single line by computing the line-to-continuum ratios [8], viz. T_e from any one of the four Balmer series $H\alpha$, $H\beta$, $H\gamma$, and $H\delta$ lines studied in this work. $H\alpha$ and $H\beta$ have been investigated previously for T_e determination from line-to-continuum ratios and 2-point Boltzmann plots [9]. Here, $H\gamma$ and $H\delta$ are examined for temperature diagnostic including use of 4-point Boltzmann plots. Moreover, of interest are applications of the laboratory diagnostic to the analysis stellar astrophysics white dwarf stars [10].

2. EXPERIMENTAL DETAILS

The experimental arrangements have been communicated previously [9,10], but a summary is included as well in this work. Laboratory laser-plasma measurements employ a pulsed, Q-switched, Nd:YAG laser device (Q-Smart 850 Quantel laser) that is operated at a pulse-width of 6 ns and a pulse energy of 850 mJ at the wavelength of 1064 nm. Laser-induced optical breakdown is generated by focusing 150 mJ per pulse of ir fundamental radiation to achieve an irradiance of the order of 1 TW/cm^2 in a cell containing ultra-pure hydrogen gas at a pressure of 0.76×10^5 Pa (11 psi).

A crossed Czerny-Turner spectrometer (Jobin Yvon 0.64 m triple spectrometer) of 0.64-nm focal length disperses the emission spectra. The pulsed radiation is focused into the cell with the beam propagating from the top and parallel to the vertical 100 µm spectrometer slit.

The spectral resolution amounts to 0.1 nm for the selected 1200 g mm^{-1} holographic grating following corrections of the wavelength variation along the slit direction [11]. Of the order of 24-nm spectral coverage is accomplished for the 1024 pixels along the wavelength-dimension.

3. RESULTS AND DISCUSSION
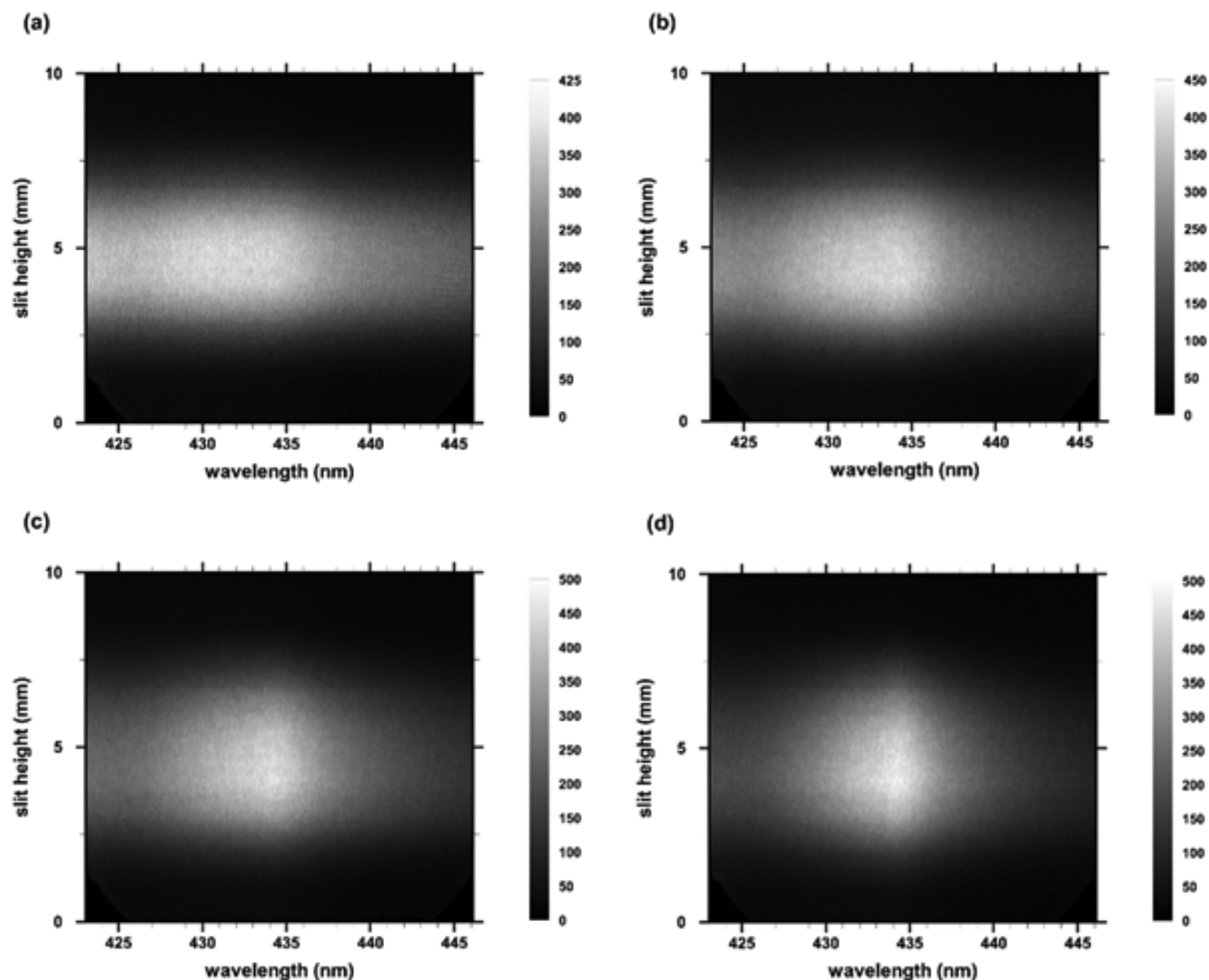
Figure 1: Hydrogen Hγ lines. Time delays (a) 100 ns, (b) 150 ns, (c) 200 ns, and (d) 275 ns

Figures 1 and 2 display time-resolved plasma spectra of Hγ and Hδ, respectively. The laser-plasma experiments [9] accumulate spectra from 100 consecutive laser-sparks in a hydrogen gas cell at a pressure of 0.76×10^5 Pa (11 psi).
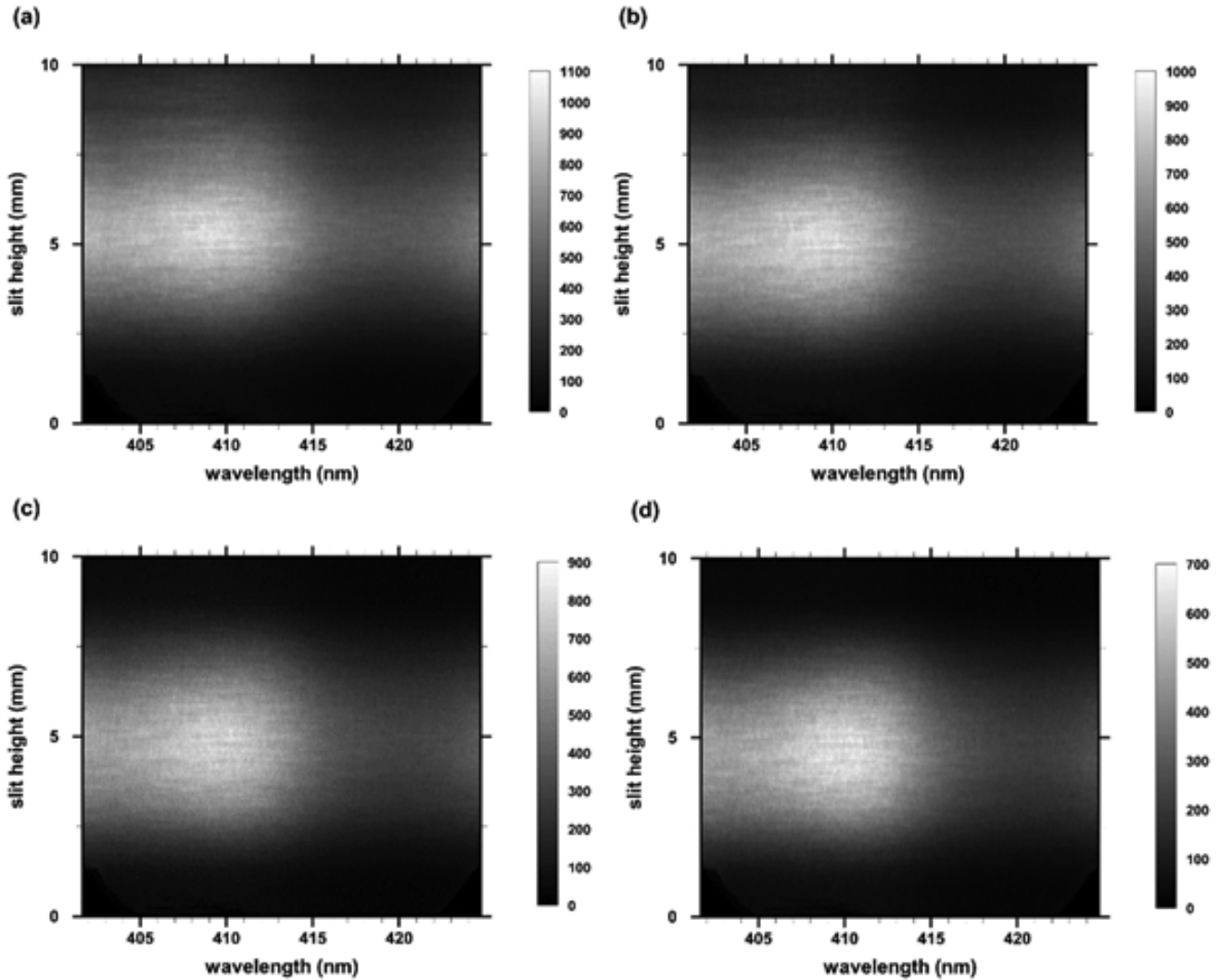
Figure 2: Hydrogen Hδ lines. Time delays (a) 100 ns, (b) 150 ns, (c) 200 ns, and (d) 275 ns

In the experiments, the laser beam propagates parallel to the slit, from top to bottom The displayed data, captured with a 5-ns gate width, are corrected for detector background and wavelength sensitivity. Wavelength calibration is accomplished with standard pen-ray light sources. The image values represent spectral radiance in arbitrary units, but with retained relative units for the different time delays and Balmer series lines. Fig. 1(a) displays Hγ (at 434.07 nm) at the low-wavelength side of the image, background contributions from Hδ (at 410.17 nm) and contributions from free-electron radiation. Fig. 1(d) indicates diminished background contributions due to Hδ. Analogously, Figure 2(a) shows Hδ with contributions from Hγ at the high wavelength side of the image. On the low wavelength side but outside the recorded spectral window, the indicated contributions are likely from Hε (at 397.01 nm) and are noticeable for all time delays in Figure 2. The full-width half-maximum (FWHM) values are extracted from the data for determination of electron densities as a function of time delay, and the integrated, significantly broadened line area is evaluated together with the 10-nm continuum.

Previously reported experimental results [9,10] use a grey-scale representation obtained from spectral-radiance data versus wavelength and slit height. For completeness, Figures 3 and 4 display Hα and Hβ maps using an analogous gray-scale.
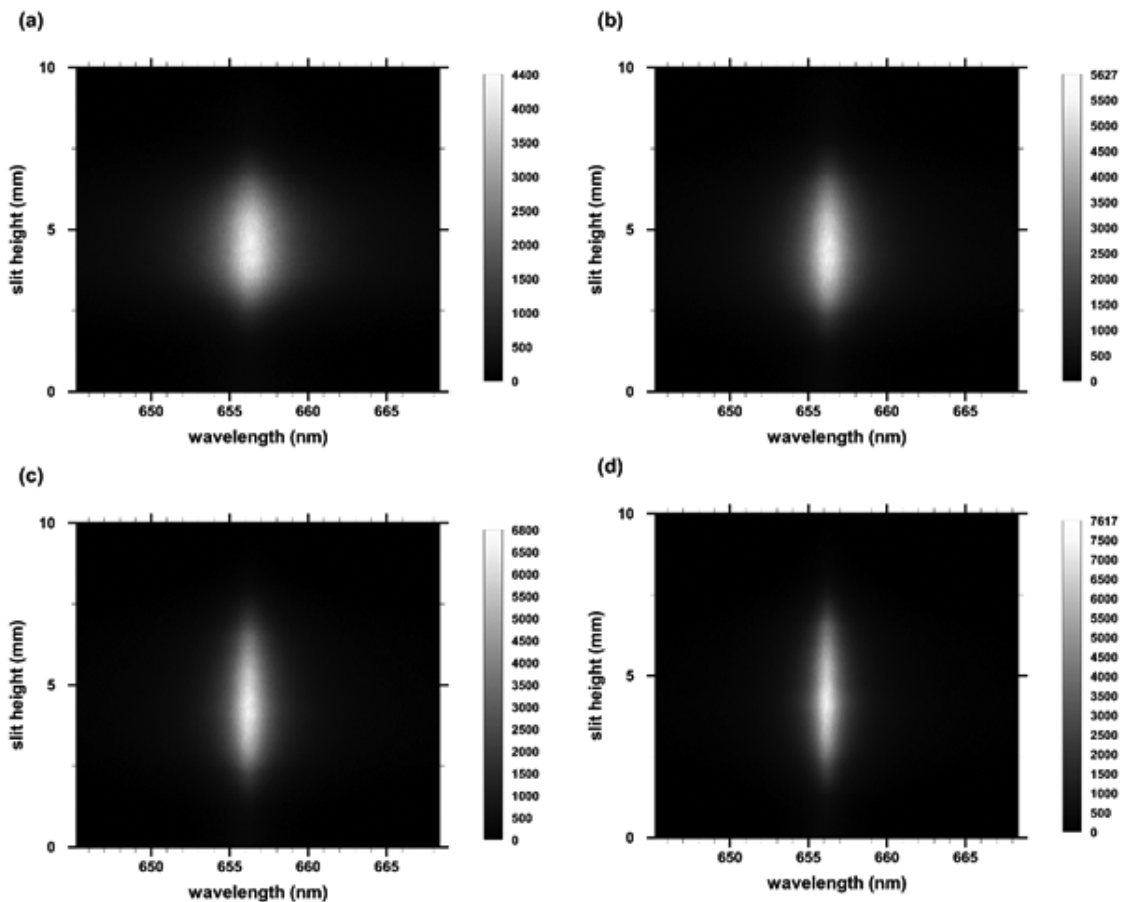
Figure 3: Hydrogen Hα lines. Time delays (a) 100 ns, (b) 150 ns, (c) 200 ns, and (d) 275

Results for the Hβ and Hα and analysis were presented previously [9,10]. Electron densities from Hβ agree with those from Hα [9,10]. Averages of the spatially resolved data along the slit yield spectra that appear similar to those recorded with a linear diode array [11,12].

The recorded Hγ and Hδ maps reveal expected variations along the slit dimension. This work reports analysis of the spectra displayed in Figures 1 and 2. Published line shapes [3] are utilized for determination of electron density. The Hγ and Hδ tables [3] are only available up to electron densities of 10^{17} cm^{-3} with temperatures up to 20 kK, but the tables usually show a weak temperature dependence. Both Hβ and Hδ show the typical dip [13] at the center wavelength also obtained from Stark effect computations [14].
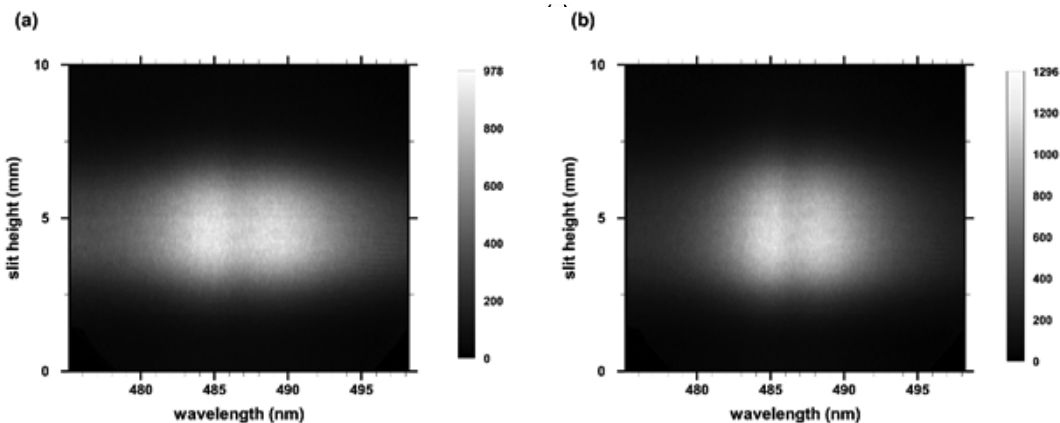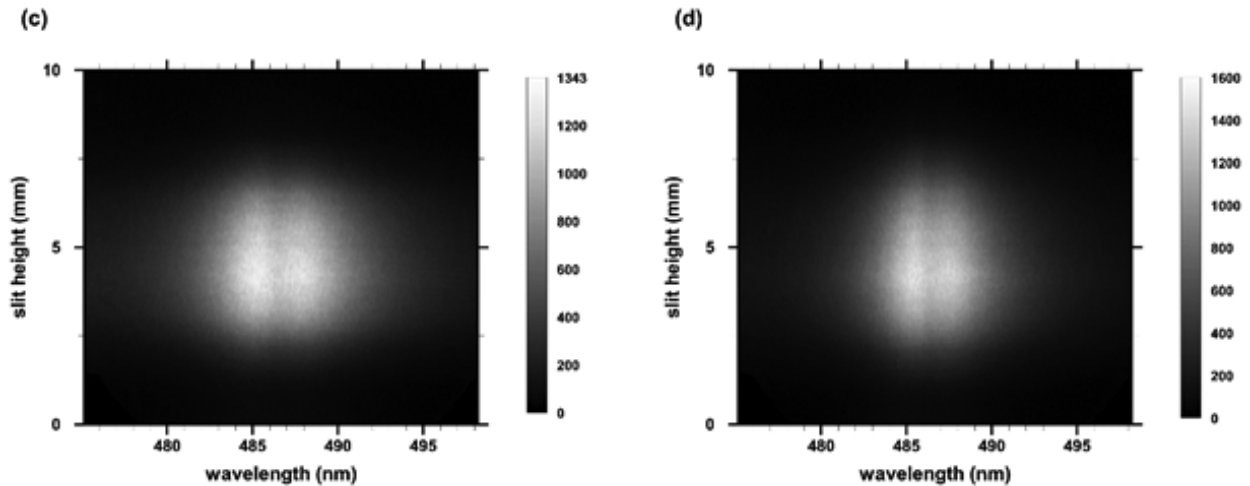
Figure 4: Hydrogen Hβ lines. Time delays (a) 100 ns, (b) 150 ns, (c) 200 ns, and (d) 275

Analysis of the recorded spectra encompasses determination of temperature from the integrated line-to-continuum ratios. Electron density measurements utilize FWHM and for Hβ and Hδ peak-separation. However, the Hδ peak-separation method is applied in analysis of experiments in 0.136-atm:0.136-atm H_2:N_2 gas mixtures (not reported here) that show electron densities in the range of 0.1 to 1×10^{17} cm^{-3} for time delays longer than those for the 0.75-atm H_2 experiments addressed in this work.

Figure 5 illustrates the line-to-continuum ratios and corresponding temperatures. The theoretical ratios of integrated line to 10-nm continuum ratios are recalculated [8], and the experimental data are added with error bars. The results for Hγ and Hδ agree with previously communicated Hα and Hβ results [9].
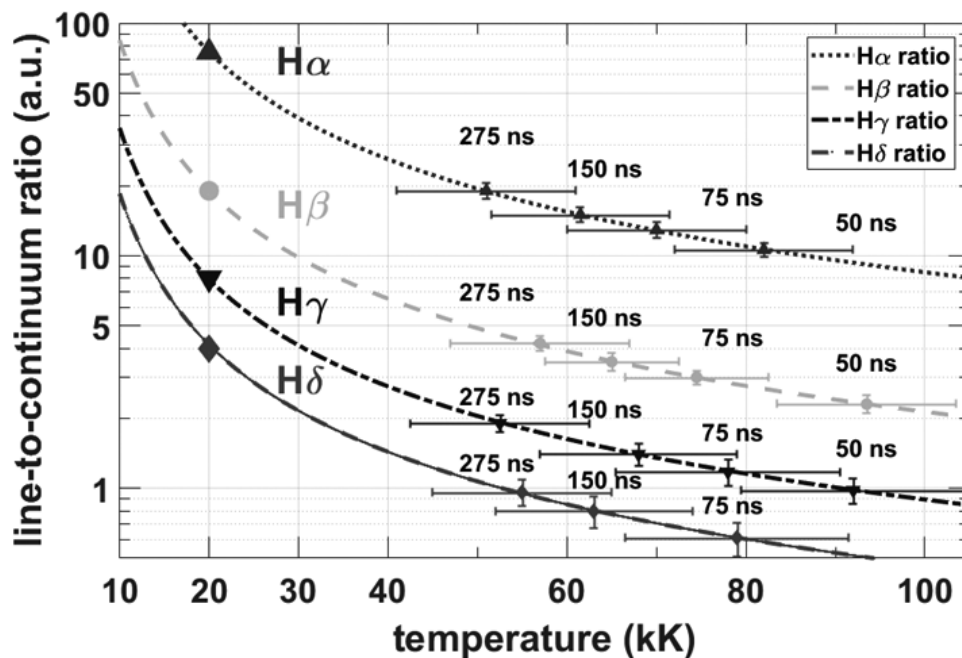
Figure 5: Computed and measured line-to-continuum ratios for selected time delays. Computed ratios of 75, 19, 8, and 4 are highlighted for Hα, Hβ, Hγ, and Hδ, respectively, at 20 kK.

Figures 6(a) and 6(b) show Boltzmann plots [15,16] and inferred temperature for time delays of 275 ns and 150 ns, respectively. The error bars reflect uncertainties in determination of the baseline.
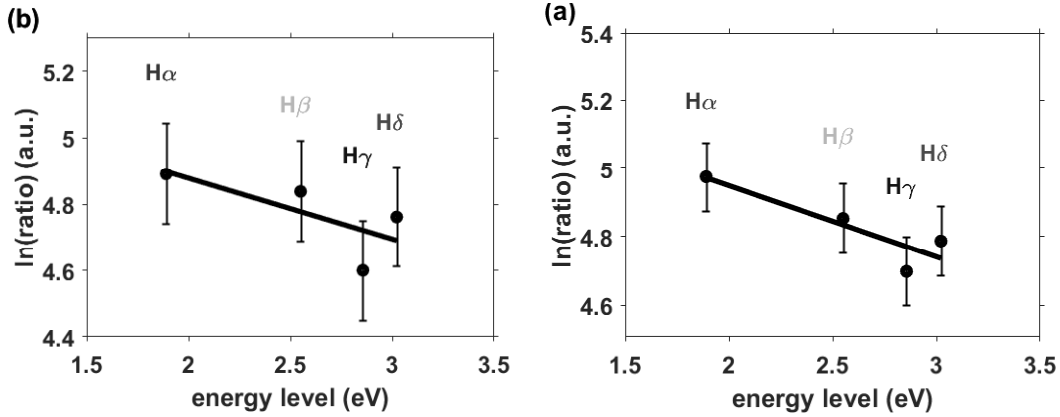
Figure 6: Boltzmann plots. (a) T = 55 kK, time delay: 275 ns. (b) T = 64 kK, time delay: 150 ns.

The Boltzmann plot utilizes the natural logarithm of the Boltzmann distribution for determination of the temperature,

$$\ln\left\{\frac{I_{ul}\lambda_{ul}}{g_u A_{ul}}\right\} = -\left\{\frac{E_u[eV]}{T[eV]}\right\} + \ln C, \tag{1}$$

where the integrated line intensities, I_{ul}, are determined in the experiment. The wavelengths, λ_{ul}, are 656.28 nm, 486.14 nm, 434.05 nm, and 410.17 nm, with degeneracies, g_u, 18, 32, 50, and 72. Transition probabilities, A_{ul}, are $4.410 \times 10^7 \, s^{-1}$, $0.8419 \times 10^7 \, s^{-1}$, $0.2530 \times 10^7 \, s^{-1}$, and $0.09732 \times 10^7 \, s^{-1}$. The excitation energies, E_u, are 1.89 eV, 2.55 eV, 2.856 eV, and 3.022 eV for Hα, Hβ, Hγ, and Hδ respectively. The constant, lnC, is not used − only the slope determines the temperature. Figure 6a and 6b display ln {ratio} = ln { $I_{ul} \lambda_{ul} / g_u A_{ul}$} versus E_u.

The deviation from a straight-line Boltzmann plot is likely due to fluid-dynamic expansion of the plasma kernel during the first 300 ns. However, temperatures from line-to-continuum ratios and Boltzmann plots agree, see Figure 5. There are expected density variations across the slit height, but the analysis evaluates averages of the displayed spectra. The analysis in this work is based on the measured line-of-sight data. Application of integral inversions for Hã and Hä lines are expected to reveal lateral temperature and density variations, analogous to Abel inversions commnicated for Hα and Hβ [17,18].

Electron densities are evaluated from the FWHM. For practical reasons, Lorentzian fitting is applied to find the FWHM of the experimental spectra. From log-log fitting of Hγ and Hδ tables in the range of 0.1 - 1 × 10^17 cm^{-3}, one obtains for FWHM of Hγ, $\Delta\lambda_\gamma$, for FWHM of Hδ, $\Delta\lambda_\delta$,

$$\Delta\lambda_\gamma[nm] = 6\left(\frac{N_e[cm^{-3}]}{10^{17}}\right)^{0.72}, \tag{2}$$

$$\Delta\lambda_\delta[nm] = 10\left(\frac{N_e[cm^{-3}]}{10^{17}}\right)^{0.67} \tag{3}$$

and the Hδ peak-separation, $\Delta\lambda_{\delta\text{-}ps}$, in the range of $0.1 - 1 \times 10^{17}$ cm^{-3} amounts to

$$\Delta\lambda_{\delta-ps}[nm] = 2\left(\frac{N_e[cm^{-3}]}{10^{17}}\right)^{0.62} \tag{4}$$

In this work, density determinations are exclusively from FWHM of the first four Balmer series lines. Future work should address density determination from Hδ peak-separations that become clearly distinguishable for electron densities in the range of 0.1 - 1×10^{17} cm^{-3}, but for longer time delays than 275 ns.

At the time delay of τ = 275 ns, the FWHM for Hγ and Hδ are 9.1 ± 2 nm and 14.8 ± 2 nm, respectively. From Equations (2) and (3) one finds electron densities of $1.78 \pm 0.4 \times 10^{17}$ cm^{-3} from Hγ and $1.8 \pm 0.3 \times 10^{17}$ cm^{-3} from Hδ. The estimated error bars are primarily due to errors in determining the baseline for the measured line profiles in the 24 nm spectral window selected for each Balmer series line. However, the Hγ and Hδ values would need to be extrapolated as the formulas are determined from Stark tables [3] that are valid up to 1×10^{17} cm^{-3}. Yet extrapolating the formulae for Hγ and Hδ yields results that would be consistent with electron densities obtained from Hα and Hβ lines [9,10], namely, 1.9×10^{17} cm^{-3}.

4. CONCLUSIONS

The Balmer Hα, Hβ, Hγ, and Hδ lines appear well-suited for determination of electron temperature from the line-to-continuum ratios. Boltzmann plot temperaures from measured, line-of-sight plasma emission spectra are in agreement with temperatures obtained from each of the four Balmer lines. The deviations from straight lines in the Boltzmann plots are likely due to the shock-wave driven plasma expansion for time delays in the range of 25 to 275 ns, and for a hydrogen gas density of 0.76×10^5 Pa. Electron temperatures inferred from all four lines are in the range of 90 kK to 40 kK for time delays of 75 to 275 ns, respectively, from optical breakdown.

The Hδ line shapes appear not double-peaked for the investigated electron densities that are larger than 1×10^{17} cm^3, however, experiments not reported here would show double-peaked Hδ line shapes for electron densities in the range of 0.1 to 1×10^{17} cm^{-3}. Detailed analysis of the spatial variation along the axial direction of the laser-plasma, or along the slit height, is expected to yield electron density variations consistent with the formation of the shock that emanates from the site of optical breakdown.

References

[1]   G.I. Taylor. *Proc. Roy. Soc. A* 201, 175 (1950).

[2]   M.A. Gigosos, M. Á. González, V. Cardeñoso. *Spectrochim. Acta B At. Spectrosc.* 58, 1489 (2003).

[3]   H.R. Griem. *Spectral Line Broadening by Plasmas*, Academic Press: Cambridge, MA, USA, 1974.

[4]   J. Holtsmark, *J. Ann. Phys.* 58, 577 (1919).

[5]   R.E. Greene, Jr. R.E. *The Shift and Shape of Spectral Lines*, Pergamon Press: Oxford, UK, 1961, Chap.4, pp. 118–193.

[6]   E. Oks. *Diagnostics of Laboratory and Astrophysical Plasmas Using Spectral Lineshapes of One-, Two-, and Three-Electron Systems*, World Scientific: Singapore, 2017, pp. 1-47.

[7]   W.L. Wiese. Line Broadening. In *Plasma Diagnostic Techniques*, Huddlestone, R.H., Leonard, S.L., Eds.; Academic Press, New York, NY, USA, 1965; pp. 265–317.

[8]   H.R. Griem. *Plasma Spectroscopy*, McGraw Hill: New York, NY, USA, 1964.

[9]   C.G. Parigger, C.M. Helstern, K.A. Drake, G. Gautam. *Int. Rev. At. Mol. Phys.* 8, 73 (2018).

[10] C.G. Parigger, K.A. Drake, C.M. Helstern, G. Gautam. *Atoms* 6, 6030036 (2018).

[11] C.G. Parigger, A.C. Woods, M.J. Witte, L.D. Swafford, D.M. Surmick. *J. Vis. Exp.* 84, e51250 (2014).

[12] C.G. Parigger, D.H. Plemmons, E. Oks. *Appl. Opt.* 42, 5992 (2003).

[13] M. Ivkovic, N. Konjevic, Z.J. Pavlovic. *J. Quant. Spectrosc. Radiat. Trans.* 54, 1 (2015).

[14] E. Schrödinger. *Ann. Phys.* 385, 437 (1926).

[15] W.L. Wiese. *Spectrochim. Acta Part B: At. Spectrosc.* 46, 831 (1991).

[16] G. Cristoforetti, A. De Giacomo, M. Dell'Aglio, S. Legnaioli, E. Tognoni, V. Palleschi, N. Omenetto. *Spectrochim. Acta Part B: At. Spectrosc.* 65, 86 (2010).

[17] C.G. Parigger, G. Gautam, D.M. Surmick. *Int. Rev. At. Mol. Phys.* 6, 43 (2015).

[18] C.G. Parigger, D.M. Surmick, G. Gautam. *J. Phys.: Conf. Ser.* 810, 012012 (2016).